ingegneria sismica
International Journal of Earthquake Engineering
Anno XLIII - Num. 2 - 2026

Research on coupling relationship mining of energy economic system and evaluation of low carbon policy effect

Jiong Wu[1,*]

[1] Yinchuan University of Energy, Yinchuan, 750100, Ningxia, China

SUMMARY: *With the development of digital energy governance, reliable measurement of energy economic coupling and low-carbon policy effects requires heterogeneous data evidence. This paper constructs a multi-source data mining framework for provincial energy, industry, economy and carbon indicators. The unified coding module converts 26 indicators in 30 regions from 2011 to 2023 into standardized time feature sequences. The coupled identification module measures the strength, direction and stability of the interaction of energy consumption, economic output, technology input and emission intensity. On this basis, the low-carbon policy effect evaluation model is constructed, and the low-carbon policy variables are mapped into the coupling state and the carbon emission reduction response. In the experiments of 10,140 region-year-indicator feature samples, the proposed model achieves 0.913 recognition accuracy, 0.887 F1-score and 6.42% MAE in coupling recognition and effect measurement. In the coupling strength fitting task, compared with the SVM, Random Forest and LSTM baselines, the MAE is reduced by 14.8%, 11.6% and 7.9%, respectively. The results provide data support for the evaluation of low-carbon policy effect and regional differentiated policy adjustment.*

KEYWORDS: *Multi-source data mining; Energy economic system; Coupling identification; Low carbon policy assessment*

1 Introduction

Under the background of the simultaneous advancement of the "double carbon" goal and digital energy governance, the energy economy system shows the characteristics of multivariate linkage and cross-regional transmission. Energy, economic and emission indicators do not simply change synchronously, but form coupled states on different time scales. After the low-carbon policy enters the economic operation, it will change the combination relationship of energy allocation, industrial output and emission response, and the statistical table is difficult to reveal the association path between the variables. The data mining method can transform the scattered energy, economic, policy and carbon emission data into a unified feature sequence, and form an evaluation link in the feature screening, association calculation and error test, which provides support for the coupling relationship mining of energy economic system and the evaluation of low-carbon policy effect.

The research has provided the foundation from the perspective of energy forecasting and carbon emission modeling. Ağbulut studied transport-related energy demand and CO2 emission forecasting in Turkey and compared the performance of different machine learning algorithms in emission trend estimation [1]. Aras and Van proposed an interpretable

*macbookfv@163.com
https://doi.org/10.65102/is2026904 Published: 30 April, 2026

prediction framework for energy consumption and CO2 emissions, which puts prediction errors and variable contributions into the same analysis process [2]. Faruque et al. conducted a comparative analysis of carbon dioxide emission prediction and showed the difference in accuracy of different algorithms under the condition of sample fluctuation [3]. Khalil et al. studied the application of machine learning, deep learning and statistical analysis in building energy consumption prediction to provide reference for energy data modeling [4]. Olu-Ajayi et al. used deep learning and other machine learning techniques to predict residential building energy consumption, and verified the ability of nonlinear models to depict energy consumption fluctuations [5]. Olu-Ajayi et al. proposed an energy performance prediction method for building design stage, so that energy decision-making can be estimated based on data models [6]. Mhlanga analyzed the application of artificial intelligence and machine learning in energy consumption and production in emerging markets, indicating that the algorithm model is suitable for extracting operation rules of energy systems [7]. Sadeghian Broujeny et al. studied the influence of exogenous data on energy consumption prediction of university office buildings and pointed out that meteorological and operational variables would change the model output [8]. Pierre et al. compared the effects of ARIMA, LSTM, GRU and their hybrid models in peak power consumption prediction, reflecting the recognition ability of time series network for peak fluctuations [9]. Olu-Ajayi et al. summarized the application boundaries of data-driven tools in building energy consumption prediction, providing a basis for multi-source data processing and model selection [10].

The above results mainly focus on energy consumption prediction, carbon emission estimation or building energy consumption scenarios, and the joint description of the internal coupling relationship of the energy economy system and the effect of low-carbon policies still needs to be refined. The energy economic system contains continuous numerical indicators and policy intensity indicators, and it is difficult to distinguish the real relationship between energy structure adjustment, economic output change and emission intensity reduction if only low carbon policies are used as ordinary explanatory variables. Based on multi-source data mining, this paper constructs a coupling relationship identification model of energy economic system, and standardizates and codes energy consumption, industrial added value, technology input, green investment, carbon emission intensity and low-carbon policy intensity to form a two-dimensional region-time sample matrix. The model calculates variable correlation, direction consistency and coupling stability in the feature layer, and establishes policy effect index mapping in the evaluation layer to measure the changes in energy efficiency, economic output and carbon emission response before and after the implementation of the policy. In the experimental part, the performance of the model is verified by regional sample data, and compared with traditional statistical models and commonly used machine learning models, the effect of the model is evaluated from the aspects of recognition accuracy, error level and the ability to describe regional differences. This method can provide data basis for digital evaluation of energy economic system and low-carbon policy adjustment.

2 Related work

As energy operation data, industrial economic data, carbon emission accounting data and policy implementation data continue to enter the digital management platform, the research of energy economy system gradually shifts from single indicator statistics to relationship recognition under multi-source data. There is an obvious linkage relationship between total energy consumption, energy intensity, industrial added value, technology input and carbon emission intensity. After the implementation of low-carbon policies, the changes of these

variables are not only reflected by a single emission decline, but also reflected by the coupling state changes between energy allocation, economic output and emission response. Traditional statistical analysis can describe the change trend of variables, but it lacks support in multi-dimensional feature coding, nonlinear relationship mining and regional difference identification. Machine learning, time series modeling and data mining methods can extract stable features from high-dimensional energy economic samples, and use error test, model comparison and index mapping to complete policy effect measurement. Therefore, it has gradually become an important technical path for energy economic system coupling relationship mining and low-carbon policy evaluation.

Afzal et al. studied the application of multilayer perceptron neural network auxiliary model in building energy consumption prediction, and compared the influence of different optimization algorithms on prediction error. The results show that the optimization algorithm can improve the fitting effect of neural network in nonlinear energy consumption data [11]. Afzal et al. further proposed a variety of neural network assisted building energy consumption prediction and optimization methods, and compared different network structures and optimization algorithms, indicating that the choice of model structure would directly affect the stability of energy consumption estimation [12]. Shahcheraghian and Ilinca studied UBC campus energy consumption analysis and optimization, and used advanced machine learning technology to depict the correlation between meteorological variables and energy consumption changes, which provided a reference path for modeling external driving factors of energy systems [13]. Gorzałczany and Rudziński proposed a residential building energy consumption prediction method combining fuzzy system and evolutionary optimization, which makes the model have strong interpretability while maintaining the prediction accuracy [14]. Matos et al. proposed a power consumption prediction and management system for renewable energy communities, and used the prediction results for energy scheduling and management decisions [15]. Koukaras et al. studied the comparison of machine learning models in short-term load forecasting of buildings, and analyzed the prediction errors and applicable scenarios of different algorithms [16].

In the direction of energy efficiency prediction and load optimization, the research strengthens time series data modeling and intelligent decision attributes. Powrźnik and Szcześniak studied the predictive analysis application of machine learning in home energy consumption optimization, emphasizing that the algorithm results can serve energy efficiency management [17]. Mosetlhe and Yusuff proposed a residential energy utilization prediction method based on regression machine learning scheme, and used a variety of regression models to estimate household energy consumption changes [18]. Anan et al. proposed a household perception energy consumption prediction model for smart buildings, which used LSTM and time series data to characterize the impact of human behavior on energy consumption [19]. Moghimi et al. studied load optimization in the islanding mode of interconnected buildings, and proposed a deep hybrid machine learning method to deal with the complex mapping between building load and operating state [20]. Zabin et al. proposed the PredXGBR short-term power load forecasting framework, which applied machine learning methods to short-term power demand estimation, reflecting the computational advantages of gradient boosting model in load forecasting [21]. The above studies show that the predictive modeling of energy-related data has shifted from single statistical fitting to multi-source feature coding, nonlinear mapping and model comparison verification. Table 1 collates the research objects, methods, and applicable boundaries of the relevant results.

Table 1: Summary of related studies on modeling energy economic systems

Research Object	Author	Method	Advantage	Applicable Boundary
Energy consumption prediction	Afzal et al.	Multilayer perceptron and optimization algorithms	Suitable for nonlinear energy consumption fitting	Sensitive to parameter combinations
Building energy consumption optimization	Afzal et al.	Comparison of multiple network structures	Enables comparison of different network performances	Limited cross-regional interpretability
Campus energy analysis	Shahcheraghian and Ilinca	Machine learning and meteorological correlation analysis	Able to identify the influence of exogenous variables	Limited embedding of policy variables
Residential energy consumption prediction	Gorzałczany and Rudziński	Fuzzy system and evolutionary optimization	Balances accuracy and interpretability	Requires a stable sample structure
Energy community management	Matos et al.	Machine learning-based prediction and management system	Supports electricity consumption management	More oriented toward operational scheduling
Short-term load forecasting	Koukaras et al.	Comparison of machine learning models	Facilitates algorithm performance screening	Insufficient expression of system coupling
Household energy efficiency	Powroźnik and Szcześniak	Predictive analytics model	Oriented toward energy efficiency management	Limited participation of economic variables
Residential energy utilization	Mosetlhe and Yusuff	Regression-based machine learning	Suitable for estimating energy-use trends	Weak expression of nonlinear relationships
Smart building energy consumption	Anan et al.	LSTM time-series model	Captures the temporal influence of occupant behavior	Policy effects are not further discussed
Connected building load	Moghimi et al.	Deep hybrid machine learning	Suitable for complex operational mapping	Insufficient regional economic linkage
Short-term electricity load	Zabin et al.	PredXGBR framework	Achieves good short-term prediction accuracy	Difficult to directly explain low-carbon policy responses

Existing results provide a clear algorithm reference for energy consumption prediction, load estimation and intelligent energy management. However, the research objects mostly

focus on buildings, families, campuses or electric community scenarios, and the variable organization is mainly based on energy consumption, weather, human behavior and operation status. The coupling relationship mining of energy economic system needs to deal with indicators such as energy consumption, industrial output, technology input, carbon emission intensity and policy intensity at the same time, and the data structure is closer to cross-regional time series panel. Single load forecasting model pays more attention to numerical forecasting accuracy, and it is difficult to fully present the linkage strength, direction consistency and dynamic stability between energy variables and economic variables. Based on this, this paper introduces multi-source data coding, coupling feature construction and policy effect measurement process on the basis of data-driven research, and forms a relationship identification framework for regional energy economic system, so that the evaluation of low-carbon policy effects can be based on computable and traceable coupling features.

3 Coupling relationship identification model of energy economic system based on multi-source data mining

3.1 Coupled feature construction based on multi-source data coding of energy economy

The identification of coupling relationship in energy economy system needs to establish a stable data input structure. Regional energy consumption, industrial output, technology input, carbon emission intensity, green investment and low-carbon policy intensity come from different statistical cali-borations, and the original data are different in dimension, time granularity and fluctuation range. If directly input into the model, the feature scale difference will amplify the impact of high-dimensional indicators and weaken the expression of low-volatility policy variables. In order to adapt to the subsequent data mining and coupling identification tasks, this paper constructs the multi-source data coding process of energy economy, and transforms the original regional panel data into a unified region-time feature matrix.

In order to eliminate the dimension differences of different indicators and make the energy, economic and policy variables enter the unified calculation space, the original indicators are normalized in this paper. The normalized indicators not only retain the annual change trend, but also compress the impact of extreme values. The calculation process is shown in the following equation:

$$\tilde{x}_{r,t,k} = \frac{x_{r,t,k} - \min(x_k)}{\max(x_k) - \min(x_k) + \varepsilon} \tag{1}$$

Here, $x_{r,t,k}$ represents the k original index of region r in year t; $\tilde{x}_{r,t,k}$ represents the normalized index value; $\max\ x_k)$ and $\min(x_k)$ represent the maximum and minimum value of the k index in the whole sample, respectively; ε is the smoothing term. This formula is used to unify the index scale, so that different dimensional variables such as total energy consumption, industrial added value, and carbon emission intensity can enter the same feature space.

Fig. 1 shows the complete process of energy economy multi-source data from the collection end into the feature space. In the figure, the left side shows five types of data sources: energy consumption, economic output, carbon emission, technology input and policy intensity; the middle side shows missing value repair, time alignment, outlier screening and

normalized coding modules; the right side shows the output of regional annual sample matrix. This process makes the data from different sources complete registration under the uniform year coordinates, and avoids the deviation of coupling relationship caused by inconsistent statistical cycle between energy data and economic data.

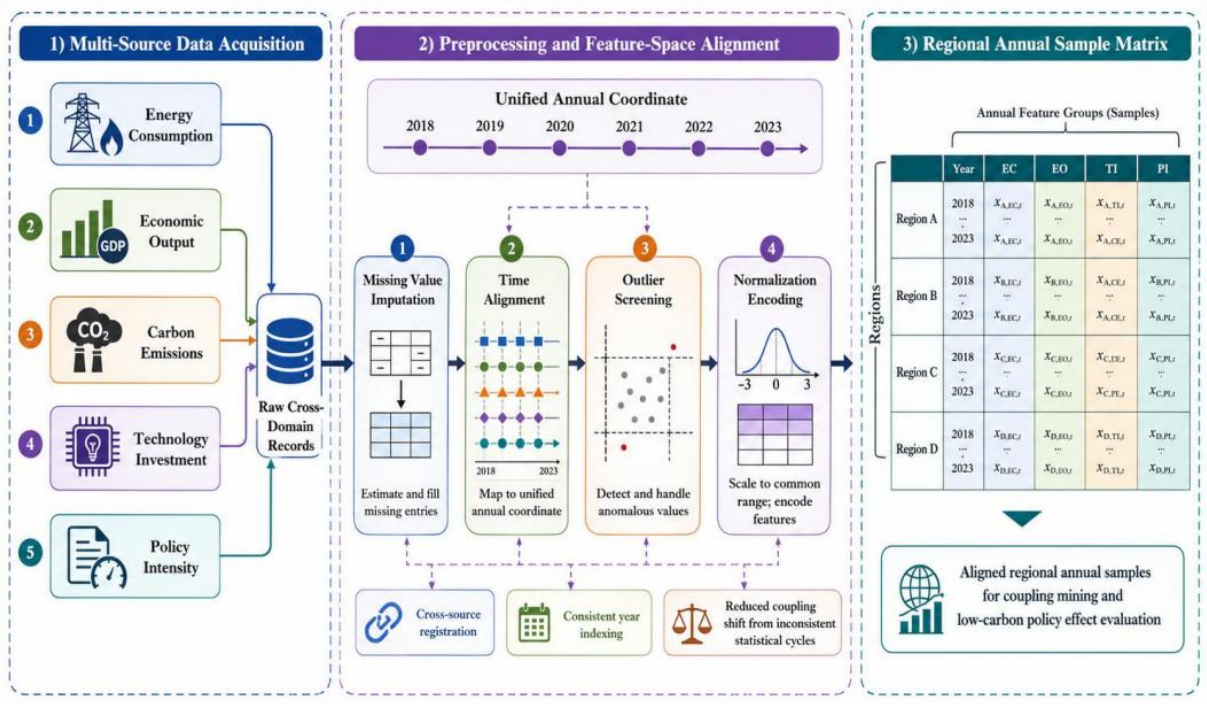

Figure 1: Energy economy multi-source data coding process

After completing the normalization of indicators, the regional annual samples need to be transformed from dispersed variables to fixed-length feature vectors. This vector carries the synchronous state of energy, economy, carbon emission and policy variables, and is the basic input for subsequent coupling feature calculation. Its construction is shown in the following equation:

$$z_{r,t} = [\tilde{x}_{r,t,1}, \tilde{x}_{r,t,2}, \ldots, \tilde{x}_{r,t,K}] \tag{2}$$

Here, $z_{r,t}$ represents the multi-source coding vector of region r over year t, and K represents the number of indicators involved in the coding. The vector organizes data in a fixed index order, which can avoid feature position drift during model training and make samples from different regions and years comparable.

Fig. 2 shows the generation structure of the coupled feature matrix. The energy subsystem indicators and the economic subsystem indicators enter the feature grouping layer respectively. The system calculates the correlation strength between variables in the sliding time window, and then embeds the carbon emission intensity and policy intensity as constraint variables into the matrix. In the figure, "energy characteristic group-economic characteristic group-emission constraint group-policy adjustment group" together form the coupling relationship calculation link, so that the model can not only identify the synchronous change between energy and economy, but also record the state difference after the entry of low-carbon policy.

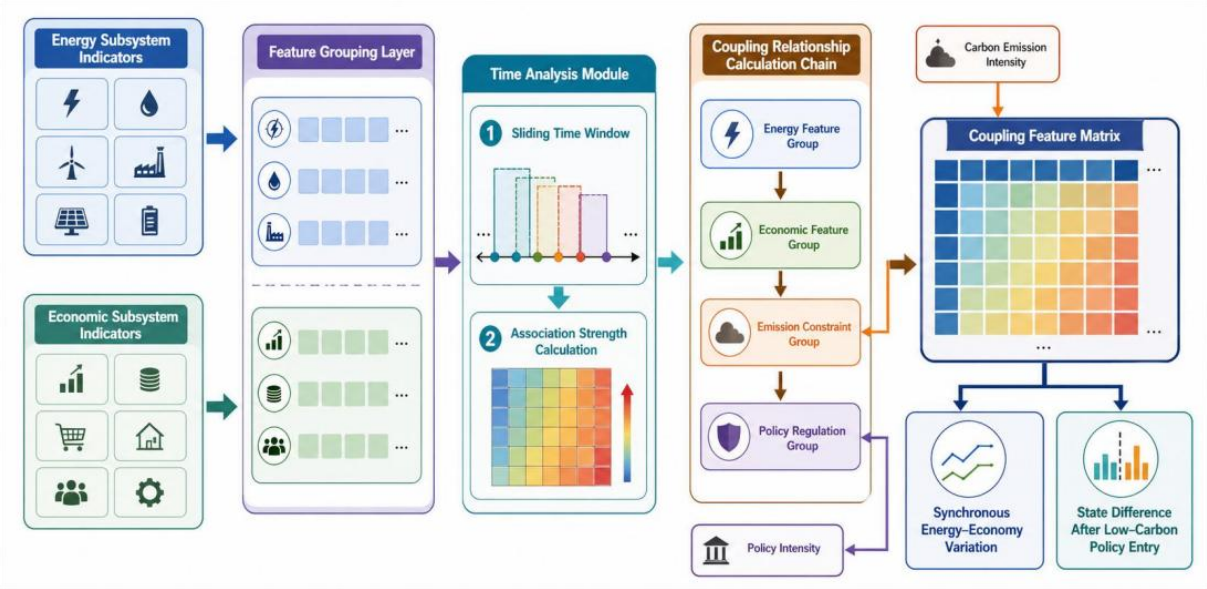

Figure 2: Energy economy coupling characteristic matrix construction process

In order to depict the local linkage relationship between energy indicators and economic indicators, the sliding window correlation calculation method is used in this paper, so that the model can identify the consistency and deviation degree of variable changes in adjacent years. The calculation process of window correlation matrix is as follows:

$$R_{i,j}^{(r,t)} = \frac{\sum_{\tau=t-q}^{t}(\tilde{x}_{r,\tau,i} - \bar{x}_{r,i})(\tilde{x}_{r,\tau,j} - \bar{x}_{r,j})}{\sqrt{\sum_{\tau=t-q}^{t}(\tilde{x}_{r,\tau,i} - \bar{x}_{r,i})^2}\sqrt{\sum_{\tau=t-q}^{t}(\tilde{x}_{r,\tau,j} - \bar{x}_{r,j})^2 + \varepsilon}} \tag{3}$$

where $R_{i,j}^{(r,t)}$ represents the correlation strength between index i and index j in the window near year t of region r, q represents the length of the sliding window, and $\bar{x}_{r,i}$ and $\bar{x}_{r,j}$ represent the mean value of the corresponding index in the window. The formula is used to extract the stage linkage characteristics between energy consumption and industrial output, and between technology input and emission intensity.

After obtaining the local correlation matrix, it is necessary to further calculate the comprehensive coupling strength between the energy subsystem and the economic subsystem. This index is used to measure the coordination state between energy input and economic output, and provide the basic state quantity for policy effect evaluation. The calculation process is shown in the following equation:

$$C_{r,t} = \frac{2\sqrt{E_{r,t}G_{r,t}}}{E_{r,t} + G_{r,t} + \varepsilon} \tag{4}$$

Here, $C_{r,t}$ represents the energy economic coupling strength of region r in year t, $E_{r,t}$ represents the comprehensive coding value of the energy subsystem, and $G_{r,t}$ represents the comprehensive coding value of the economic subsystem. This formula can reflect the matching degree between energy input and economic output, and a higher value indicates that the energy economic system exhibits a stronger synergistic state in that year.

It is difficult to judge whether the variable changes in the same direction only by relying on the coupling strength. Therefore, this paper further sets up the direction consistency index

to identify the same direction relationship between energy variables and economic variables in annual changes. The calculation process is shown in the following equation:

$$D_{r,t} = \frac{1}{K_e K_g} \sum_{i=1}^{K_e} \sum_{j=1}^{K_g} \mathbb{I}\left(\Delta x_{r,t,i} \cdot \Delta x_{r,t,j} > 0\right) \tag{5}$$

where, $D_{r,t}$ represents the direction consistency coefficient, K_e represents the number of energy indicators, K_g represents the number of economic indicators, $\Delta x_{r,t,i}$ represents the annual change of indicators, and $\mathbb{I}(\cdot)$ is the indicator function. The formula can determine whether there is a synchronous change between energy consumption, energy intensity, economic output and technology input, and avoid the simple correlation coefficient to mask the direction difference.

In order to reduce the interference of short-term fluctuations on the coupling results, it is necessary to measure the stability of multi-year coupling states. The stability index can reflect the continuity degree of regional energy economic relations in the time series, and its calculation process is shown as follows:

$$S_r = 1 - \frac{\sqrt{\frac{1}{T}\sum_{t=1}^{T}(C_{r,t} - \bar{C}_r)^2}}{\bar{C}_r + \varepsilon} \tag{6}$$

Here, S_r represents the coupling stability of region r, T represents the number of observation years, and $\bar{C}_r$ represents the average coupling strength of region r in the full time period. The formula identifies whether the regional energy economic system has a continuous and stable linkage structure by constraining the discrete degree of coupling strength.

Low carbon policy variables are not ordinary background variables, but an important regulating factor affecting the state of energy economy. In order to make policy information enter the model calculation link, this paper encodes the low-carbon policy intensity, green investment level and industrial constraint intensity as policy features, and the calculation process is shown in the following equation:

$$P_{r,t} = \lambda_1 L_{r,t} + \lambda_2 I_{r,t} + \lambda_3 M_{r,t} \tag{7}$$

Here, $P_{r,t}$ represents the policy feature value of region r at year t, $L_{r,t}$ represents the low-carbon policy intensity, $I_{r,t}$ represents the green investment level, $M_{r,t}$ represents the industry constraint intensity, and λ_1 to λ_3 represent the corresponding weights. This formula converts policy implementation information into numerical variables that can be read by the model, so that low-carbon policies can participate in energy economic coupling relationship identification.

Fig. 3 presents the final output structure of the coupling characteristics of the energy economy system. In the figure, the left part retains the regional annual basic coding vector, the middle part is integrated into the four relationship features of local correlation matrix, coupling strength, direction consistency and stability, and the right part is embedded into the low-carbon policy intensity, green investment level and industrial constraint intensity to form the policy feature layer. All kinds of features are not added directly, but enter the unified output in the order of "basic status-relationship expression-policy adjustment" to form the regional annual coupling feature vector. The structure can simultaneously preserve the

original state of the energy economic system, the variable linkage relationship and the policy intervention information, so that the subsequent low-carbon policy effect evaluation model can directly read the complete system characteristics and avoid the information loss caused by repeated coding.

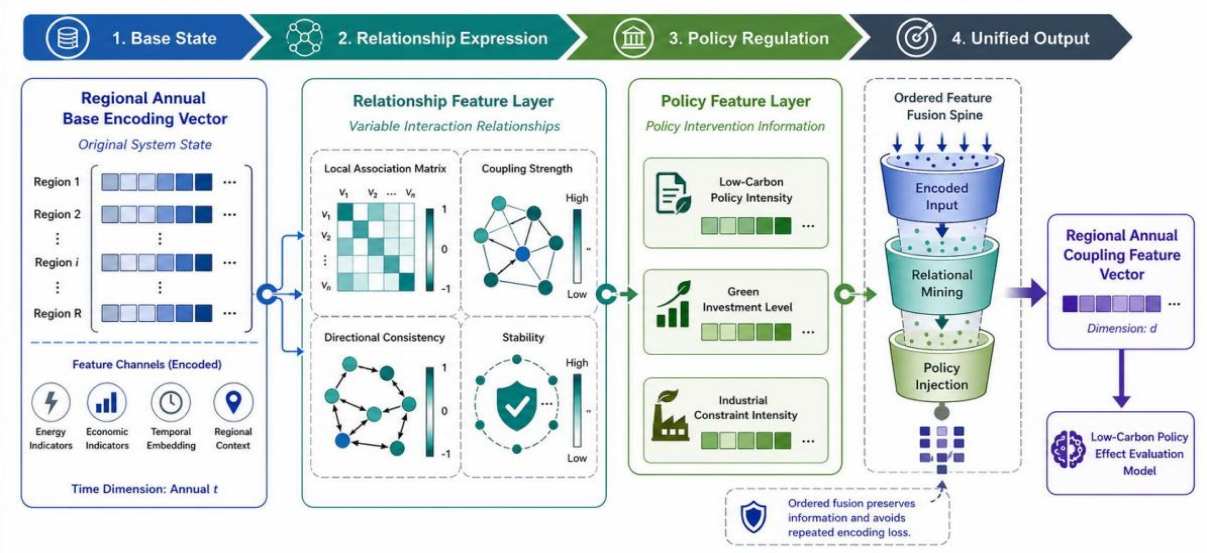

Figure 3: Energy economy system coupling characteristic output structure

After completing the basic coding, coupling strength calculation and policy variable embedding, this paper concatenates various features into the final coupling feature vector, which is used to undertake the subsequent effect evaluation task. The expression is shown in the following equation:

$$F_{r,t} = [z_{r,t}, R_{i,j}^{(r,t)}, C_{r,t}, D_{r,t}, S_r, P_{r,t}] \tag{8}$$

Here, $F_{r,t}$ represents the final coupling feature vector of region r at year t; $z_{r,t}$ represents the underlying multi-source coding vector; $C_{r,t}$, $D_{r,t}$, S_r and $P_{r,t}$ represent the coupling strength, direction consistency, stability and policy characteristics, respectively. The vector integrates energy, economic, emission and policy information into the same computational structure, so that the subsequent models can evaluate the effect of low-carbon policies in a unified feature space.

After the above processing, the multi-source indicators in the energy economy system are transformed from scattered statistical data into computable, comparable and traceable coupled features. The coding result not only retains the regional time series change, but also expresses the relationship strength between energy economic variables and the policy embedding state, which provides a stable input for the construction of low-carbon policy effect evaluation indicators and models in the next section.

3.2 Indicator construction and model design for low-carbon policy effect evaluation

The evaluation of the effect of low-carbon policies should not only stop at the simple comparison of carbon emission values before and after the implementation of policies, but also need to put energy allocation, economic output, technology input and emission intensity into the same calculation structure. The regional energy economic system will produce

multi-dimensional response under the action of policy, energy efficiency may be improved, industrial output structure may be adjusted, and carbon emission intensity may also show a phased decline or lag change. If the evaluation model only focuses on a single emission reduction index, it is easy to ignore the coupling state changes inside the energy economic system. In order to ensure the computability and interpretability of the evaluation results, this paper constructs a low-carbon policy effect evaluation model based on policy input, system response, benchmark status, index weight and regional differences. The model incorporates policy intensity, green investment, industrial constraints, energy efficiency, economic output and carbon emission intensity into a unified feature space, and forms a policy effect evaluation link for regional samples through benchmark response generation, effect difference measurement and comprehensive score output.

In order to unify the expression of low-carbon policy input and energy economic system response, the model organizes policy characteristics, coupling states and changes into response vectors to support difference measurement, and its expression is shown in the following equation:

$$u_{r,t} = [P_{r,t}, C_{r,t}, \Delta E_{r,t}, \Delta G_{r,t}, \Delta B_{r,t}] \tag{9}$$

Here, $u_{r,t}$ represents the policy response vector of region r in year t; $P_{r,t}$ represents the policy characteristics; $C_{r,t}$ represents the energy economic coupling strength; $\Delta E_{r,t}$, $\Delta G_{r,t}$, and $\Delta B_{r,t}$ represent the changes in energy efficiency, economic output and carbon emission intensity, respectively. This vector enables policy input and system response to be expressed in the same unit, which facilitates the reading of multidimensional effects.

Fig. 4 shows the construction path of the policy effect indicator. The left side of the figure is the policy input layer, including policy intensity, green investment level, industry constraint intensity and technology input intensity. The middle part is the system state layer, which receives the calculation characteristics of energy efficiency, economic output, carbon emission intensity and coupling strength. The right side is the effect measurement layer, which matches the policy input with the system response to form four types of indicators: emission reduction response, economic constraint, energy efficiency change and coupling improvement. The structure puts policy variables, energy economic status and emission results into the same link, so that the effect score has a clear source and index boundary.

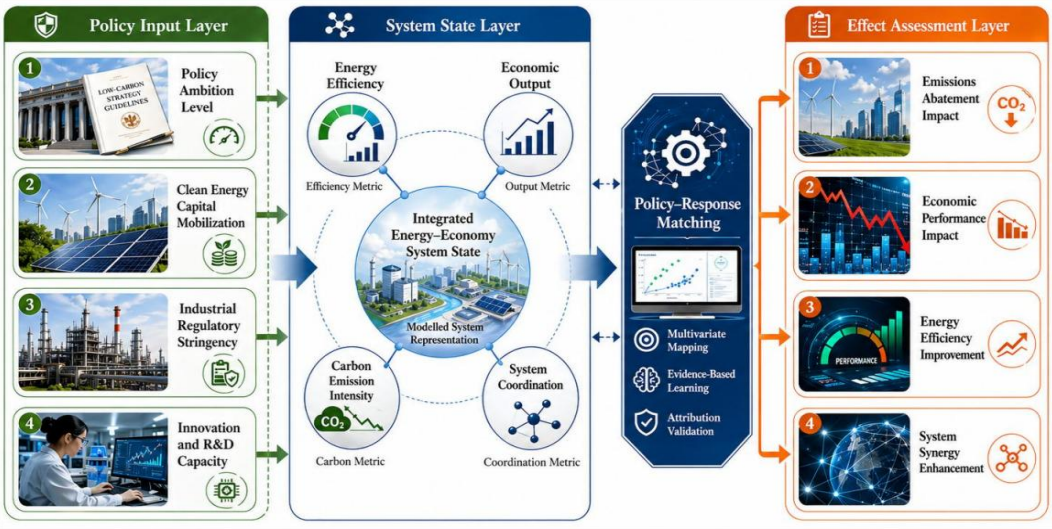

Figure 4: Construction path of low carbon policy effect indicators

In order to construct the reference state required for policy effect measurement, the model generates the benchmark response value based on historical coupling characteristics, regional structural attributes and time trends, and the calculation process is shown in the following equation:

$$\hat{y}_{r,t}^{0} = g_{\theta}(F_{r,t-1}, s_r, \tau_t) \tag{10}$$

Here, $\hat{y}_{r,t}^{0}$ represents the benchmark response value of region r in year t, $g_{\theta}(\cdot)$ represents the mapping function with parameter θ, $F_{r,t-1}$ represents the coupling characteristics of the last period, s_r represents the structural attributes of the region, and τ_t represents the time trend. This formula is used to form a reference path that enables the actual response to be measured differently from comparable states.

After obtaining the actual response and the baseline response, the policy effect is represented by the deviation value between the two types of responses, and the independent results of different indicator dimensions are retained. The calculation process is shown in the following equation:

$$e_{r,t,m} = y_{r,t,m} - \hat{y}_{r,t,m}^{0} \tag{11}$$

Here, $e_{r,t,m}$ denote the policy effect size on the m indicator,$y_{r,t,m}$ denote the actual observed response, and $\hat{y}_{r,t,m}^{0}$ denote the benchmark response. The formula can describe the changes of energy efficiency, economic output and carbon emission intensity respectively, and avoid the comprehensive scoring to mask the differences of indicators.

In order to reduce the interference of high volatility indicators on the comprehensive results, the model assigns weights according to the policy response intensity of indicators and the volatility degree of samples. The weight generation method is shown in the following equation:

$$\omega_m = \frac{\exp(\rho_m/(\sigma_m + \varepsilon))}{\sum_{j=1}^{M} \exp(\rho_j/(\sigma_j + \varepsilon))} \tag{12}$$

Here, ω_m represents the weight of the m category indicator, ρm represents the response strength between this indicator and policy characteristics, σ_m represents the degree of sample fluctuation, and M represents the number of indicators. This formulation makes the indicators with stable response and policy sensitive obtain higher contributions, and weakens the interference of noise variables.

Fig. 5 shows the internal calculation process of the policy effect measurement model. The benchmark estimation module generates the reference response, the difference measurement module compares the deviation value between the actual response and the benchmark response, the weight distribution module adjusts the effect contribution according to the index sensitivity and fluctuation degree, and the comprehensive aggregation module outputs the policy effect value. Each module is connected in the order of "input feature-baseline response-effect difference-weight aggregation-effect output", which ensures the traceability of the results.

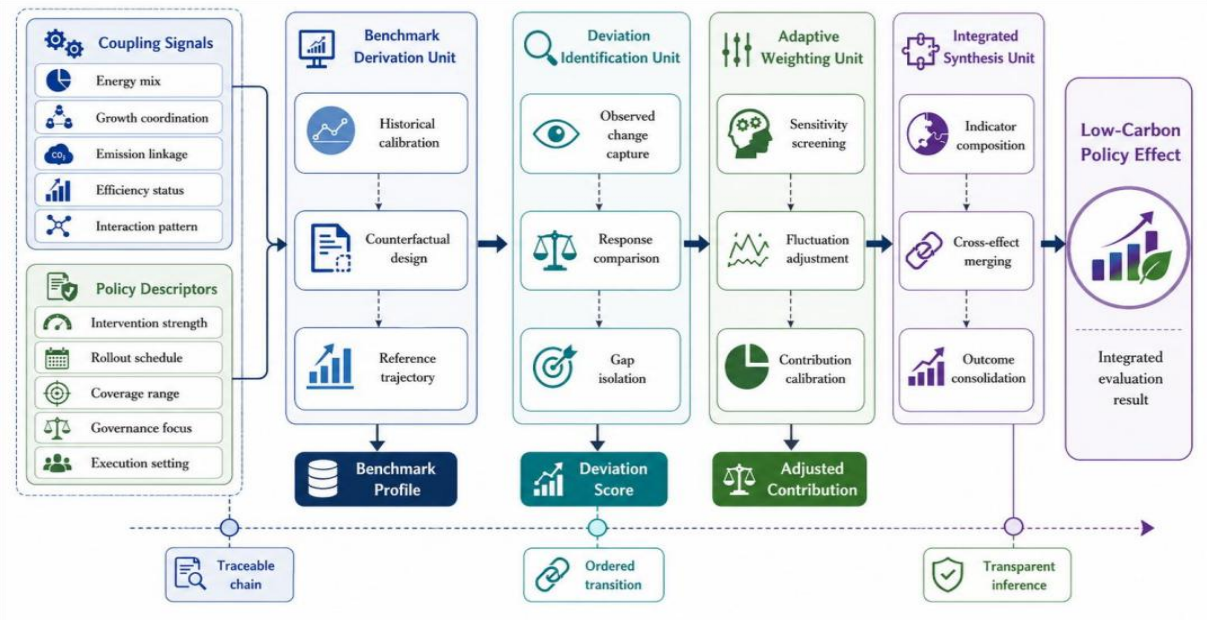

Figure 5: Process of low carbon policy effect measurement model

The comprehensive effect value is obtained by weighting multiple indicators, which not only considers the emission reduction response, but also retains the economic output and energy efficiency constraints, so that the evaluation results are in line with the analysis goal of the energy economy system, and its expression is shown in the following equation:

$$Q_{r,t} = \sum_{m=1}^{M} \omega_m \, e_{r,t,m} \tag{13}$$

Here, $Q_{r,t}$ represents the comprehensive policy effect value of region r in year t, and $e_{r,t,m}$ represents the corresponding indicator effect. This formula converts the dispersion response into a comparable result, which is convenient for the same aperture measurement in different regions and years.

In order to maintain the continuity of the model output in the time series and control the traction of abnormal samples, the model sets three constraints of fitting, smoothing and sparsity, and its loss function is shown in the following equation:

$$\mathcal{L} = \frac{1}{N}\sum_{r,t}(Q_{r,t} - \bar{Q}_{r,t})^2 + \alpha \sum_{r,t}(Q_{r,t} - Q_{r,t-1})^2 + \beta\|\theta\|_1 \tag{14}$$

Here, $\mathcal{L}$ represents the training loss, $\bar{Q}_{r,t}$ represents the calibration effect size, N represents the number of samples, α represents the temporal smoothing coefficient, and β represents the parameter sparsity constraint. The formula makes the model fit the sample effect and keep the change stable, and reduces the influence of redundant parameters.

In order to reflect the dispersion degree of policy effects in different regions, the regional difference intensity index is introduced into the model, and the comprehensive effects of each region in the same year are standardized and discrete measured. The calculation process is shown in the following equation:

$$V_t = \sqrt{\frac{1}{R}\sum_{r=1}^{R}(Q_{r,t} - \bar{Q}_t)^2} \tag{15}$$

Here, V_t represents the intensity of regional differences in year t, R represents the number of regions, and $\bar{Q}_t$ represents the average policy effect of all regions in that year. This formula is used to quantify the degree of differentiation of policy effects among regions, so that the evaluation results present both overall level and spatial differences.

Fig. 6 presents the output structure of the policy effect evaluation results. The left side shows the comprehensive effect value, coupling improvement amount, regional difference strength and index contribution degree, the middle part shows the score integration layer and regional contrast layer, and the right side outputs the policy effect score, regional difference ranking, indicator contribution explanation and response path record. Instead of a single total score output, the structure retains effect size, coupling change, regional dispersion degree and indicator contribution, so that the evaluation results can be used for regional comparison and also illustrate the impact of policy variables on energy efficiency, economic output and carbon emission response.

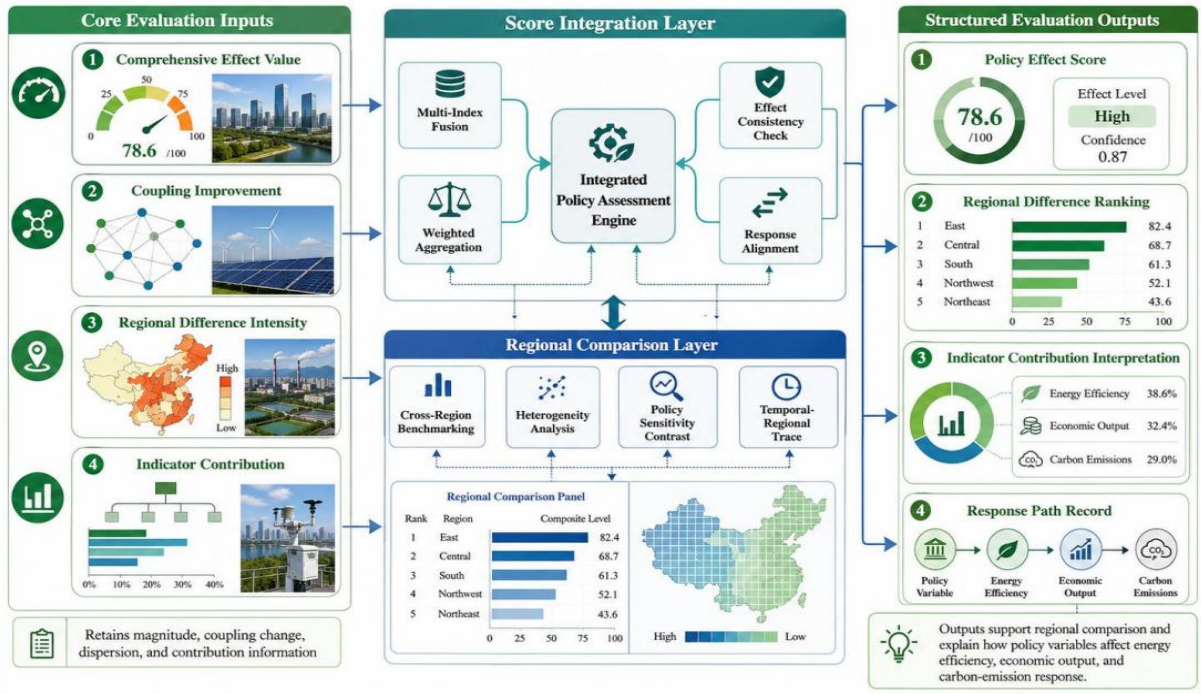

Figure 6: Output structure of low carbon policy effect evaluation

In order to form the final evaluation result, the model incorporated the comprehensive effect, coupling improvement and regional difference penalty term into the same scoring function to obtain the total score of policy effect, as shown in the following equation:

$$\Theta_{r,t} = \mu_1 Q_{r,t} + \mu_2 (C_{r,t} - C_{r,t-1}) - \mu_3 V_t \tag{16}$$

Here, $\Theta_{r,t}$ represents the final low-carbon policy effect score, $Q_{r,t}$ represents the comprehensive policy effect value, $C_{r,t-1}$ represents the improvement of coupling strength,

V_t represents the strength of regional differences, and μ_1 to μ_3 represents the weight coefficient. Policy response, coupling state change and regional differences are incorporated into the same function, so that the result reflects the emission reduction effect and the coordinated change of energy economy.

Through the above design, the low-carbon policy effect evaluation model forms a link from index input, benchmark generation, difference measurement, weight aggregation to score output. Policy variables are involved in the calculation together with energy efficiency, economic output, carbon emission intensity and coupling improvement. The intermediate variable records were kept in the model to form a reviewable data relationship among policy intensity, system response, regional differences and final score, which enhanced the interpretation of results and application stability.

4 Empirical verification of energy economic system and low-carbon policy effect based on coupling relationship identification model

4.1 Comparative performance analysis of coupling relationship identification models

In order to verify the recognition ability of the coupling relationship recognition model in the energy economic system, the experiment selects the energy, economy, industry, technology, carbon emission and low carbon policy data of 30 regions from 2011 to 2023, and constructs 10140 regional time series samples. The sample index includes 26 variables, of which the energy side includes total energy consumption, energy intensity, proportion of clean energy and energy consumption per unit output; the economic side includes industrial added value, regional product, industrial structure proportion and technology input; the low-carbon side includes carbon emission intensity, green investment level, policy intensity and industry constraint intensity. Time alignment, imputation of missing values, censoring of outliers, standardized coding, and calculation of coupled features were completed before data entered the model. The experiment used the ratio of 7∶2∶1 to divide the training set, validation set and test set, and set SVM, Random Forest and LSTM as comparison models. The evaluation metrics include Accuracy, Precision, Recall, F1-score, and MAE to test the performance of the model in coupling state discrimination, boundary sample identification, and error control. The proposed model takes multi-source coupling features as input, fuses local correlation matrix, direction consistency, stability and policy features, and identifies three types of states: high coupling, weak coupling and unbalanced coupling.

Table 2 presents the comprehensive performance of coupled state recognition. The model in this paper maintains a high level of Accuracy, Precision, Recall and F1-score, where the Accuracy is 0.913 and the F1-score is 0.887. Compared with SVM, the F1-score is increased by 0.066. Compared with Random Forest, it is increased by 0.041. Compared with LSTM, it improves by 0.021. The results show that when the coupling strength, direction consistency and stability characteristics enter the unified vector, the model can more fully identify the weak coupling and unbalanced coupling samples, and the results are closer to the operation state of the regional energy economic system.

Table 2: Comprehensive performance comparison of coupling relationship identification models

Model	Accuracy	Precision	Recall	F1-score
SVM	0.842	0.835	0.808	0.821
Random Forest	0.867	0.856	0.837	0.846
LSTM	0.885	0.878	0.855	0.866
Proposed Model	0.913	0.901	0.874	0.887

Fig. 7 shows the ROC curves of the four classes of models in the coupled state recognition task. This figure shows the model discrimination boundary by the change of false positive rate and recall rate, reflecting the stability of different algorithms in threshold movement. The AUC of the proposed model reaches 0.946, which is higher than that of SVM (0.884), Random Forest (0.902) and LSTM (0.921). The curve still keeps rising smoothly in the high recall interval, indicating that the model has a strong ability to distinguish boundary samples. LSTM is sensitive to successive year changes, but shows local shifts in regions with large fluctuations in policy intensity. SVM is limited by the boundary of the kernel function, and it is insufficient to express the nonlinear relationship between energy efficiency and carbon emission intensity.

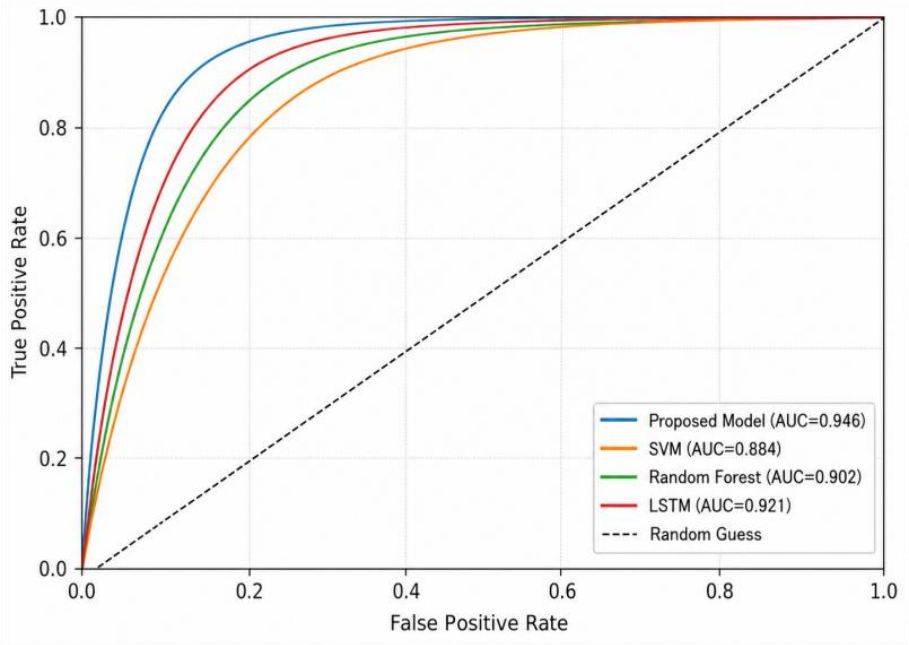

Figure 7: Coupled state identification ROC curves for four classes of models

Fig. 8 shows the confusion matrix heatmap of the proposed model on the three classes of coupling states. In the figure, the main diagonal has the darkest color, which indicates the correct recognition sample set. A total of 3260 highly coupled samples were identified, of which 3014 were correctly identified, and the recognition rate was 92.45%. There were 4186 weak-coupling samples, 3781 were correctly identified, and the recognition rate was 90.32%. A total of 2694 imbalance coupling samples were identified, and 2462 were correctly identified, with a recognition rate of 91.39%.

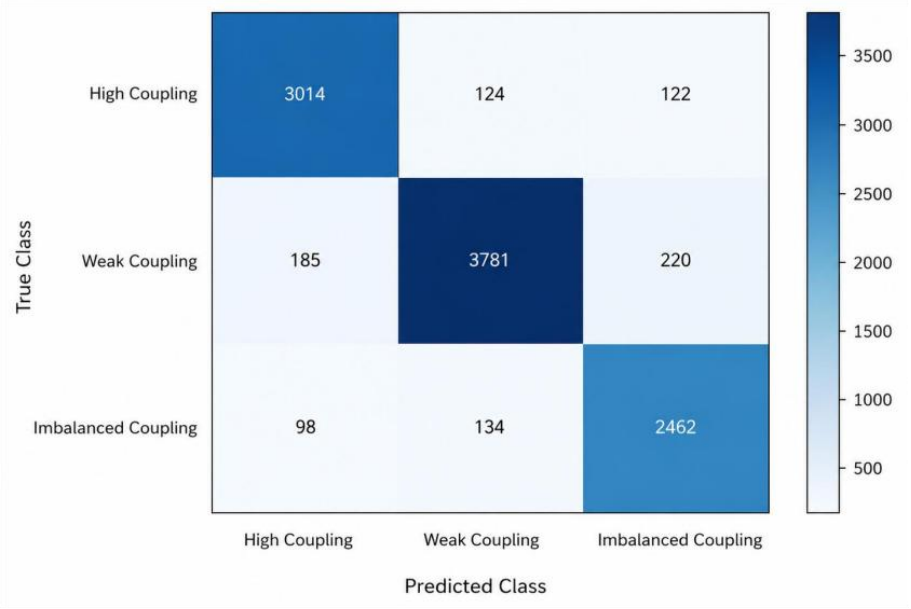

Figure 8: Heatmap of the confusion matrix for coupled state recognition of the proposed model

Table 3 presents the recognition performance after input of different feature groups. When the basic energy economic indicators enter the model, the F1-score is 0.842 and the MAE is 8.13%. After adding the local correlation matrix, the F1-score is increased to 0.861, and the MAE is reduced to 7.42%. After adding direction consistency and stability, the F1-score reaches 0.879. The complete coupling feature makes the F1-score reach 0.887, and the MAE is reduced to 6.42%. This change shows that multi-source data encoding can transform the variable synchronization relationship, direction relationship and stability relationship into learnable features.

Table 3: Recognition performance with different feature group inputs

Feature Group	Accuracy	F1-score	MAE/%
Basic energy–economic indicators	0.864	0.842	8.13
Basic indicators + local correlation matrix	0.881	0.861	7.42
Basic indicators + correlation matrix + stability	0.902	0.879	6.88
Complete coupling features	0.913	0.887	6.42

Fig. 9 shows the kernel density distribution of the four types of models on the fitting error of the coupling strength. The error of the proposed model is mainly concentrated between -0.05 and 0.06, and the peak value is close to 0, indicating that the deviation between the predicted coupling strength and the labeling result is small. SVM has a wide error distribution, forming a tail in the positive error interval. Random Forest is stable for medium and low coupling samples, but underestimated for high coupling samples. The LSTM error distribution is relatively concentrated and still shows a shift in the year of abrupt policy intensity change. The MAE of the proposed model is 6.42%, which is 14.8%, 11.6%and 7.9%lower than that of SVM, Random Forest and LSTM, respectively.

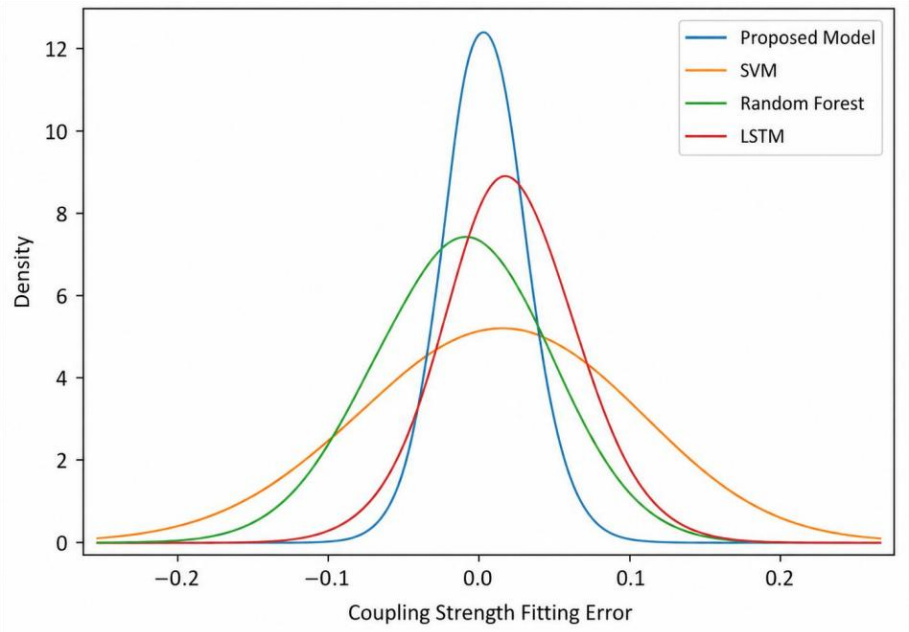

Figure 9: Coupling strength error kernel density distribution for four classes of models

Table 4 lists the stability test results under different region types. In the eastern sample, the Accuracy of the model in this paper is 0.921, and the F1-score is 0.894. The Accuracy of the middle sample is 0.909, and the F1-score is 0.883. The Accuracy of the western sample is 0.904, and the F1-score is 0.876. The Accuracy gap between the three regions is controlled within 0.017, indicating that the model does not over-rely on a certain type of regional samples. The MAE of the western region is slightly higher, which is mainly affected by the high proportion of energy production, the fluctuation of industrial structure and the lag of policy response, but the overall identification results still maintain usable stability.

Table 4: Model stability tests under different region types

Region Type	Accuracy	F1-score	MAE/%
Eastern region	0.921	0.894	6.18
Central region	0.909	0.883	6.47
Western region	0.904	0.876	6.71

Fig. 10 compares the performance of the four types of models in five dimensions of recognition accuracy, stability, error control, regional generalization and computational efficiency using radar plots. The scores of the five items of the model in this paper are 0.913, 0.902, 0.896, 0.889 and 0.874, respectively, and the contour is more balanced. LSTM is close to the proposed model in the stability dimension, but its computational efficiency score is 0.812. Random Forest has good computational efficiency, but low error control score. SVM has a simple structure and poor regional generalization ability. The multi-source coupling feature makes the model maintain a balance between accuracy and stability.

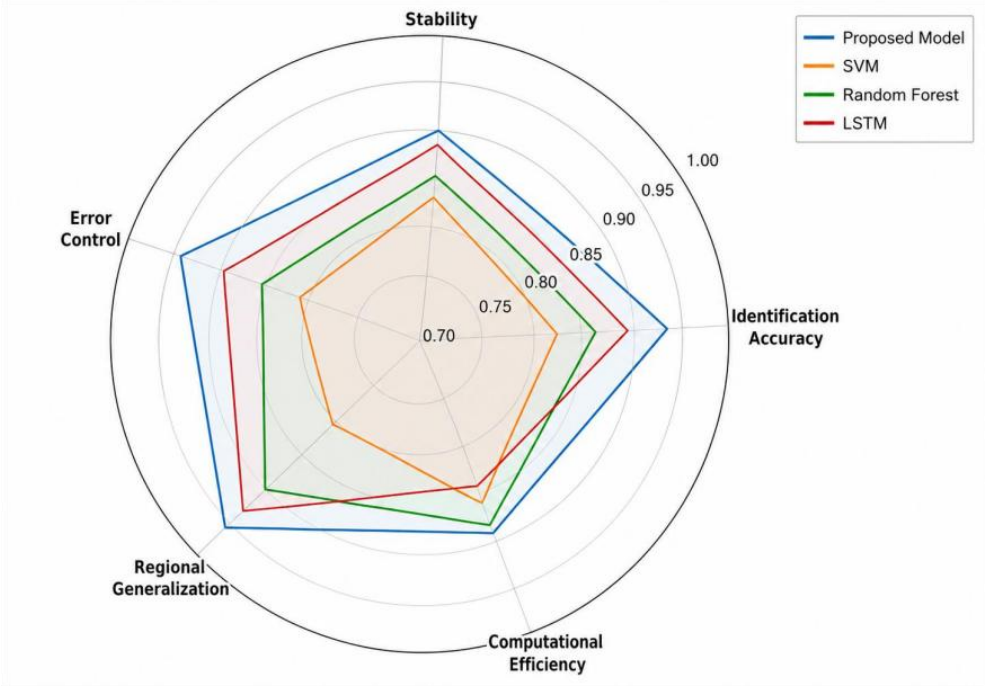

Figure 10: Multidimensional performance radar plots for four classes of models

The comprehensive results show that the proposed model is superior to the comparison models in coupling state discrimination, feature contribution utilization, error control and regional robustness. The performance advantage comes from the combined effect of multi-source data encoding, local incidence matrix, direction consistency and stability features. The model can not only identify the overall coupling state of the energy economic system, but also retain the regional differences under the change of policy intensity, which provides a credible coupling relationship input for the calculation of low-carbon policy effects.

4.2 Calculation results of low carbon policy effect and verification of regional differences

The low-carbon policy effect measurement is based on the identification results of the coupling relationship between energy and economy, and focuses on the response states of energy efficiency, economic output, carbon emission intensity and coupling improvement after the policy intensity is entered into the model. The experiment uses 10140 regional time series samples formed by 30 regions from 2011 to 2023. The model input is the coupled feature vector, and the output includes the comprehensive policy effect value, the strength of regional difference and the contribution degree of indicators. DID, Random Forest, LSTM and XGBoost are selected as comparison methods to test the performance of the model in effect measurement, error control and regional adaptability.

Fig. 11 shows the spatial and temporal distribution of the effect values of low-carbon policies in different regions from 2011 to 2023. The figure takes regional type and year as two dimensions to reflect the changes in the comprehensive effects of energy efficiency, economic output and carbon emission intensity after the policy intensity is entered into the model. Before 2015, the effect values of most regional policies were concentrated between 0.31 and 0.46, which was at a low level. After 2020, the mean value of the eastern region increased to 0.67, the central region reached 0.62, the northeast region increased to 0.59, and the western region remained between 0.48 and 0.56. The data show that the effect of low-carbon policy is

not released synchronously in all regions, but is strongly related to the energy structure, industrial base and green investment level.

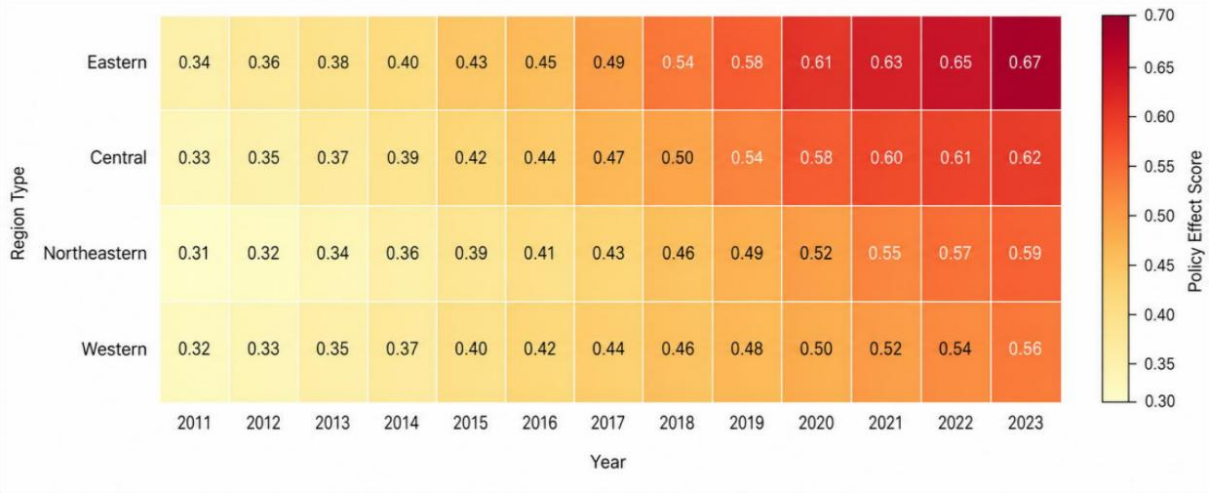

Figure 11: Spatio-temporal thermal distribution of low-carbon policy effect

Table 5 shows the policy effect measurement errors of different models. The MAE of the proposed model is 6.42%, RMSE is 0.083, MAPE is 7.18%, and R-squared reaches 0.901. DID can describe the differences before and after the policy, but the expression of regional heterogeneity is weak. Random Forest is stable in fitting static variables and has insufficient time series response. LSTMS are able to capture annual variation but have limited structural explanation for policy intensity; The XGBoost error control is better than the traditional model, but it is still higher than the proposed model in the regional difference term. The data show that after coupling features and policy features enter the model together, the effect measurement results are closer to the calibrated values.

Table 5: Measurement errors of low carbon policy effects for different models

Model	MAE/%	RMSE	MAPE/%	R^2
DID	9.84	0.126	10.97	0.782
Random Forest	8.91	0.113	9.63	0.814
LSTM	7.98	0.102	8.55	0.852
XGBoost	7.41	0.096	8.02	0.871
Proposed Model	6.42	0.083	7.18	0.901

The error differences in Table 5 illustrate that policy effect measurement cannot rely only on traditional before and after comparisons. DID has a clear structure when dealing with policy shocks, but is weak in expressing nonlinear coupling relationships when facing multi-region, multi-index, and multi-year samples. Random Forest can depict the importance of static variables, but it is difficult to retain the annual conduction order. LSTMS can read temporal dependencies, but the metric contribution interpretation is not straightforward enough. The proposed model inputs coupling strength and policy features together to form a more balanced result between error compression and explanation retention.

Fig. 12 shows the distribution differences of low carbon policy effect scores in different regions. This figure is used to observe the median, degree of dispersion and abnormal fluctuations of each regional sample, so as to judge whether the policy effect is stable within the region. In the eastern region, the median was 0.66, and the interquartile range was 0.08,

indicating that the sample distribution was relatively concentrated. The median of the central region was 0.61, and the interquartile range was 0.10, indicating that the overall fluctuation was within a controllable range. In the western region, the median was 0.53, and the interquartile range was 0.14, indicating a large internal difference. The median of the Northeast region is 0.57, and the upper quartile reaches 0.64, indicating that the improvement of some samples is obvious in the later period.

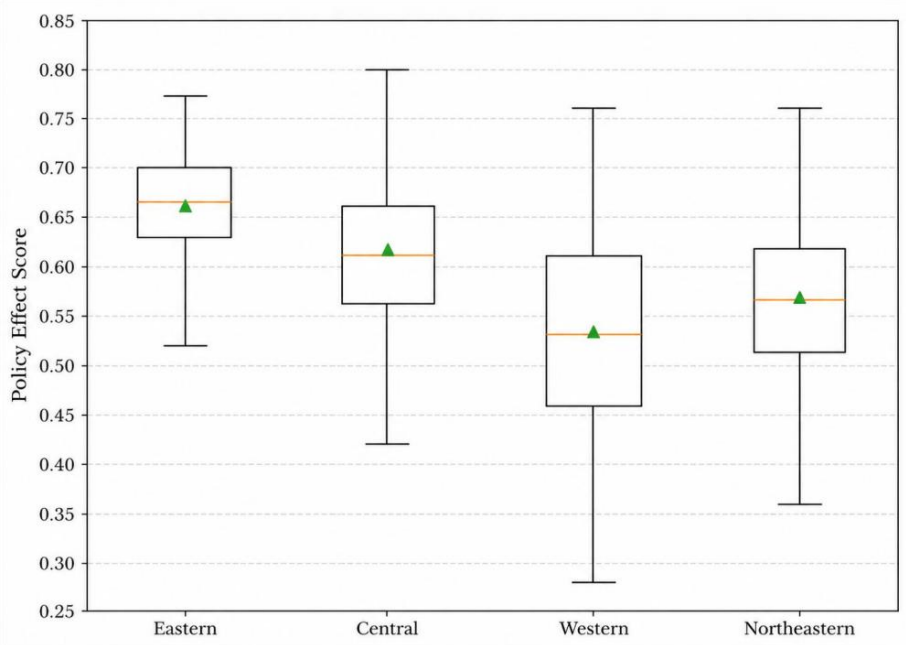

Figure 12: Boxplots of low carbon policy effect scores for different regions

Table 6 lists the system response results for different policy intensity groups. In the high intensity group, the comprehensive effect value was 0.682, the coupling improvement was 0.094, the energy efficiency change was 7.86%, and the carbon emission intensity reduction was 8.73%. The comprehensive effect value of the moderate intensity group was 0.594, and the carbon emission intensity decreased by 6.41%. In the low intensity group, the comprehensive effect value was 0.487, and the coupling improvement was only 0.041. With the increase of policy intensity, energy efficiency and coupling improvement show synchronous enhancement, indicating that there is a relatively stable mapping relationship between policy variables and energy economy state.

Table 6: Effect measurement results for different policy intensity groups

Policy Intensity Group	Comprehensive Effect Value	Coupling Improvement	Energy Efficiency Change/%	Carbon Emission Intensity Reduction/%
High-intensity group	0.682	0.094	7.86	8.73
Medium-intensity group	0.594	0.067	6.02	6.41
Low-intensity group	0.487	0.041	4.15	4.36

Fig. 13 shows the contribution structure of each index in the calculation of low carbon policy effect. This figure depicts the composition of model output results from five dimensions: energy efficiency, carbon emission intensity, economic output, green investment and industrial constraints. The contribution degree of energy efficiency was 0.31, and the

contribution degree of carbon emission intensity was 0.28, and the two items together reached 0.59, which constituted the main source of policy effect calculation. The contribution degree of economic output is 0.19, indicating that the model retains the economic operation constraint when calculating the emission reduction effect. The contribution degree of green investment and industrial constraint were 0.13 and 0.09, respectively, which mainly reflected the adjustment effect of policy input on regional differences.

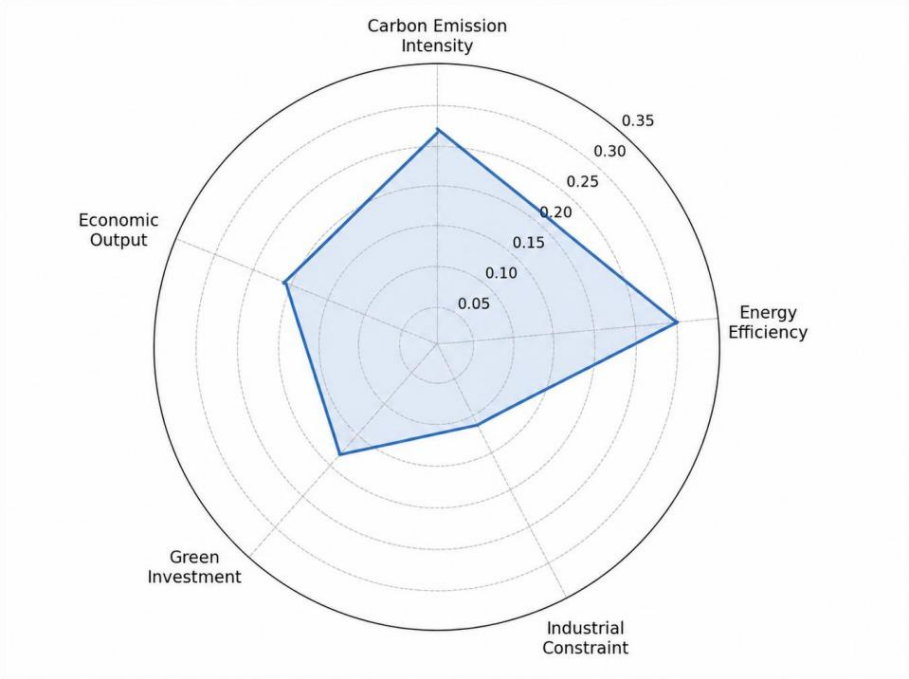

Figure 13: Radar plot of low carbon policy effect indicator contribution

To test the influence of each computing module on the measured results, Table 7 sets the ablation experiment. After removing the coupling strength, MAE increased to 7.56% and F1-score decreased to 0.862. After removing the direction consistency, the regional difference error increases to 0.081. After removing the policy feature layer, R-squared decreased to 0.846. After removing the temporal smoothing constraint, the annual effect size fluctuation increases. The full model performs more stable in MAE, F1-score, R-² and regional difference error, indicating that the coupling strength, direction consistency, policy characteristics and time constraints jointly support the effect measurement results.

Table 7: Ablation experiments of the low carbon policy effect measurement model

Model Setting	MAE/%	F1-score	R^2	Regional Difference Error
Without coupling strength	7.56	0.862	0.861	0.074
Without directional consistency	7.21	0.871	0.872	0.081
Without policy feature layer	7.88	0.858	0.846	0.079
Without temporal smoothing constraint	7.34	0.866	0.865	0.086
Complete model	6.42	0.887	0.901	0.058

Table 8 presents the robustness results under different Windows of years. In the 2011-2018 window, the MAE of the model was 6.78%, and the average effect size was 0.548. In the 2014-2021 window, MAE decreased to 6.51%, and the average effect size increased to

0.586. In the window from 2016 to 2023, the MAE is 6.39%, and the R-squared reaches 0.906. After the window is shifted back, the low-carbon policy intensity and green investment variables in the sample are more complete, and the model depicts the policy response more stably. The R-squared of the three Windows remain above 0.89, indicating that the model has strong robustness under different policy stages.

Table 8: Robustness verification under Windows of different years

Year Window	MAE/%	RMSE	R^2	Average Effect Value
2011–2018	6.78	0.089	0.891	0.548
2014–2021	6.51	0.085	0.897	0.586
2016–2023	6.39	0.081	0.906	0.612

The year window results in Table 8 illustrate that the model does not drift significantly in the different stage samples. The policy variables in the early window data were relatively sparse, and the error was slightly higher. After introducing more green investment and industry constraint information in the medium-term window, the fitting ability of the model was enhanced. The low carbon policy intensity and energy efficiency variables in the recent window are more complete, and the R^2 rises further. The average effect size of the three Windows shows an increasing trend, reflecting the cumulative response of the low-carbon policy input in the time dimension.

It can be seen from the comprehensive chart results that the effect of low carbon policy shows obvious differentiation between regions. Relying on higher technology investment and green investment intensity, the eastern region more fully released the policy effect. The performance of the central region was relatively stable, with energy efficiency improvement keeping pace with industrial output; Affected by the proportion of resource-based industries, the coupling improvement speed of the western region is relatively slow. The northeast region shows reparative growth in the later samples. The model can output effect size, index contribution, time stability and regional differences at the same time, which makes the low-carbon policy evaluation turn from single result judgment to multi-dimensional data verification, and provides a computable basis for regional differentiated policy adjustment.

5 Discussion

The identification model of coupling relationship of energy economic system constructed in this paper emplaces multi-source data coding, local correlation matrix, direction consistency, stability constraint and policy characteristics into the same calculation link, so that energy, economy, carbon emission and low carbon policies are no longer isolated indicators. The experimental results show that the model achieves 0.913 accuracy and 0.887 F1 value in coupling state recognition, which indicates that multi-source coupling features can enhance the discrimination ability of boundary samples. Compared with SVM, Random Forest and LSTM, the error distribution of the proposed model is more concentrated, and the MAE is reduced to 6.42%, indicating that feature coding and relationship measurement have strong expression ability for the nonlinear linkage of energy economic system. The calculation results of low carbon policy effects show that policy intensity, green investment and industrial constraints enter the unified feature space, which can more clearly reflect the corresponding relationship between the improvement of energy efficiency, the change of economic output and the decline of carbon emission intensity. The regional results also show that the effect size is high for the eastern and central samples, while the western sample is affected by the

structure of energy production and lags in policy response. This difference indicates that the evaluation of low-carbon policies should not only rely on a single emission reduction indicator, but should make a comprehensive judgment by combining the coupling improvement, the intensity of regional differences and the contribution of indicators. The value of the model in this paper is to transform policy effects into traceable calculation results, so that regional energy economic governance has more stable data basis. In terms of technical implementation, the model keeps intermediate variable records, which facilitates the review of index sources, parameter changes and regional response paths, and enhances the operational ability of subsequent expansion.

6 Conclusions

Focusing on the coupling relationship mining of energy economic system and the evaluation of low carbon policy effect, this paper constructs a identification and measurement framework based on multi-source data mining. The model incorporates energy consumption, industrial output, technology input, carbon emission intensity and policy intensity into a unified feature space, and forms a complete calculation link from system state identification to policy response measurement through data coding, coupling strength measurement, direction consistency constraint and policy effect scoring. The results show that the multi-source feature coding can enhance the expression ability of the relationship between energy economic variables, the coupled features can support the recognition of regional states, and the embedding of policy features can provide a clearer calculation basis for the evaluation of low-carbon policy effects. The value of our method does not lie in the prediction of individual indicators, but in the organization of energy, economic, emission and policy variables into a traceable data structure, so that regional differences, policy responses and system collaborative changes in low-carbon governance can be modeled and expressed. There are still some limitations in this paper. The samples mainly come from regional annual level statistical data, and the coverage of enterprise-level carbon emissions, real-time energy scheduling and policy implementation details is still insufficient. The model's response ability to short-cycle fluctuations and sudden industrial changes needs further verification. Future research can introduce online learning, dynamic feature update and cross-region migration mechanisms to expand the ability of multi-frequency data access, and combine interpretable artificial intelligence methods to refine the variable contribution analysis. In the future, the model can also be embedded into the energy management platform and carbon accounting system to form a continuously updated low-carbon policy evaluation interface, which provides more stable and reliable calculation support and basis for regional differentiated regulation.

Author's Profile

Jiong Wu, native to Nanjing, Jiangsu Province, holds a master's degree and the professional title of Lecturer. Graduated from Northwest Normal University, he is currently employed by Yinchuan University of Energy. His main research focus lies in regional spatial structure.

References

[1] Ağbulut Ü. Forecasting of transportation-related energy demand and CO2 emissions in Turkey with different machine learning algorithms[J]. Sustainable Production and

Consumption, 2022, 29: 141-157.

[2] Aras S, Van M H. An interpretable forecasting framework for energy consumption and CO2 emissions[J]. Applied Energy, 2022, 328: 120163.

[3] Faruque M O, Rabby M A J, Hossain M A, et al. A comparative analysis to forecast carbon dioxide emissions[J]. Energy Reports, 2022, 8: 8046-8060.

[4] Khalil M, McGough A S, Pourmirza Z, et al. Machine Learning, Deep Learning and Statistical Analysis for forecasting building energy consumption—A systematic review[J]. Engineering Applications of Artificial Intelligence, 2022, 115: 105287.

[5] Olu-Ajayi R, Alaka H, Sulaimon I, et al. Building energy consumption prediction for residential buildings using deep learning and other machine learning techniques[J]. Journal of Building Engineering, 2022, 45: 103406.

[6] Olu-Ajayi R, Alaka H, Sulaimon I, et al. Machine learning for energy performance prediction at the design stage of buildings[J]. Energy for Sustainable Development, 2022, 66: 12-25.

[7] Mhlanga D. Artificial intelligence and machine learning for energy consumption and production in emerging markets: A review[J]. Energies, 2023, 16(2): 745.

[8] Sadeghian Broujeny R, Ben Ayed S, Matalah M. Energy consumption forecasting in a university office by artificial intelligence techniques: An analysis of the exogenous data effect on the modeling[J]. Energies, 2023, 16(10): 4065.

[9] Pierre A A, Akim S A, Semenyo A K, et al. Peak electrical energy consumption prediction by ARIMA, LSTM, GRU, ARIMA-LSTM and ARIMA-GRU approaches[J]. Energies, 2023, 16(12): 4739.

[10] Olu-Ajayi R, Alaka H, Owolabi H, et al. Data-driven tools for building energy consumption prediction: A review[J]. Energies, 2023, 16(6): 2574.

[11] Afzal S, Ziapour B M, Shokri A, et al. Building energy consumption prediction using multilayer perceptron neural network-assisted models; comparison of different optimization algorithms[J]. Energy, 2023, 282: 128446.

[12] Afzal S, Shokri A, Ziapour B M, et al. Building energy consumption prediction and optimization using different neural network-assisted models; comparison of different networks and optimization algorithms[J]. Engineering Applications of Artificial Intelligence, 2024, 127: 107356.

[13] Shahcheraghian A, Ilinca A. Advanced machine learning techniques for energy consumption analysis and optimization at UBC Campus: Correlations with meteorological variables[J]. Energies, 2024, 17(18): 4714.

[14] Gorzałczany M B, Rudziński F. Energy consumption prediction in residential buildings—An accurate and interpretable machine learning approach combining fuzzy systems with evolutionary optimization[J]. Energies, 2024, 17(13): 3242.

[15] Matos M, Almeida J, Gonçalves P, et al. A machine learning-based electricity consumption forecast and management system for renewable energy communities[J]. Energies, 2024, 17(3): 630.

[16] Koukaras P, Mustapha A, Mystakidis A, et al. Optimizing building short-term load forecasting: A comparative analysis of machine learning models[J]. Energies, 2024, 17(6): 1450.

[17] Powroźnik P, Szcześniak P. Predictive analytics for energy efficiency: Leveraging machine learning to optimize household energy consumption[J]. Energies, 2024, 17(23): 5866.

[18] Mosetlhe T, Yusuff A A. Forecasting of Residential Energy Utilisation Based on Regression Machine Learning Schemes[J]. Energies, 2024, 17(18): 4681.

[19] Anan M, Kanaan K, Benhaddou D, et al. Occupant-aware energy consumption prediction in smart buildings using a LSTM model and time series data[J]. Energies, 2024, 17(24): 6451.

[20] Moghimi S M, Gulliver T A, Chelvan I T, et al. Load optimization for connected modern buildings using deep hybrid machine learning in island mode[J]. Energies, 2024, 17(24): 6475.

[21] Zabin R, Haque K F, Abdelgawad A. PredXGBR: A Machine Learning Framework for Short-Term Electrical Load Prediction[J]. Electronics, 2024, 13(22): 4521.